

Discovery of γ -ray pulsations of PSR J1835–3259B in the Globular Cluster NGC 6652

PENGFEEI ZHANG,¹ YI XING,² AND ZHONGXIANG WANG^{1,2}

¹*Department of Astronomy, School of Physics and Astronomy, Key Laboratory of Astroparticle Physics of Yunnan Province, Yunnan University, Kunming 650091, People's Republic of China; zhangpengfei@ynu.edu.cn; wangzx20@ynu.edu.cn*

²*Key Laboratory for Research in Galaxies and Cosmology, Shanghai Astronomical Observatory, Chinese Academy of Sciences, 80 Nandan Road, Shanghai 200030, People's Republic of China; yixing@shao.ac.cn*

ABSTRACT

Motivated by the newly discovery of a spin period 1.83 ms pulsar J1835–3259B in the globular cluster (GC) NGC 6652, we analyze the γ -ray data obtained with the Large Area Telescope (LAT) onboard *Fermi Gamma-ray Space Telescope (Fermi)* for the GC and detect the pulsations of this millisecond pulsar (MSP) at a 5.4σ confidence level (the weighted H-test value is ~ 41). From timing analysis of the data, a pulse profile that is similar to the radio one is established. We thus consider that we have detected the γ -ray emission of the MSP, and discuss the implications. Based on our analysis results and different studies of the sources in the GC, the observed γ -ray emission from the GC could mainly arise from this MSP, like the previous two cases the GCs NGC 6624 and NGC 6626. Assuming this is the case, the pulsar, at the GC's 9.46 kpc distance and having a spin-down luminosity of $\leq 4.3 \times 10^{35}$ ergs⁻¹, would have a γ -ray luminosity of $\simeq (5.04 \pm 0.44) \times 10^{34}$ ergs⁻¹ and a γ -ray efficiency of $\gtrsim 0.12$.

Keywords: Gamma-rays(637); Globular star clusters(656); Pulsars (1306)

1. INTRODUCTION

Globular clusters (GCs) are spherical ensembles of old stars that constitute as an important part of our Galaxy. They contain $\sim 10^5$ stars within themselves and most of them have typical ages of greater than 10^{10} year (e.g., Harris 1996). Owing to the high stellar densities and thus frequent dynamical interactions in their cores, GCs are the natural sites to form compact low-mass X-ray binaries, whose further evolution resulting in formation of millisecond pulsars (MSPs; Bhattacharya & van den Heuvel 1991). Therefore GCs can be considered as factories of MSPs. This scenario is supported by the observational facts that thus far 257 MSPs have been detected in 36 GCs within ~ 20 kpc of the Galactic center¹ and these GC MSPs constitute a fraction of $\sim 50\%$ of known MSPs in our Galaxy (Manchester et al. 2005).

Since the successful launch of the *Fermi Gamma-ray Space Telescope (Fermi)* and use of the Large Area Telescope (LAT) onboard (Atwood et al. 2009), the first case of γ -ray detection of GCs, the 47 Tuc, was reported by (Abdo et al. 2009), then followed with that of Terzan 5 by Kong et al. (2010). Now approximately 40 GCs have

been reported to have detectable γ -ray emission (Abdo et al. 2010b,a; Tam et al. 2011; Zhou et al. 2015; Zhang et al. 2016; Lloyd et al. 2018a; de Menezes et al. 2019a; Abdollahi et al. 2020; Yuan et al. 2022). It is generally considered that the γ -ray emission of GCs primarily arises from the MSPs contained within them. This consideration has been well supported by the discoveries of pulsed γ -ray emission of an individual pulsar that dominates the detected γ -ray emission of a whole GC, specifically PSR J1823–3021A in NGC 6624 (Freire et al. 2011) and B1821–24 in NGC 6626 (or M28; Wu et al. 2013; Johnson et al. 2013). Also not only the γ -ray luminosities of the GCs but also their γ -ray spectra have been analyzed to show that the emission is consistent with that arising from a number of MSPs in each GCs (Abdo et al. 2010a; Hui et al. 2011; de Menezes et al. 2019b; Lloyd et al. 2018b; Zhang et al. 2020; Song et al. 2021; Wu et al. 2022).

Recently, Gautam et al. (2022) reported the discovery of a 1.83 ms MSP, PSR J1835–3259B, in a near-circular orbit of 28.7 hr within the GC NGC 6652. This MSP is the second one found in this GC, while the first is PSR J1835–3259A that has a spin period of 3.89 ms and is in a wide binary with orbital period 9.25 day (DeCesar et al. 2015). NGC 6652 also shows detectable γ -ray

¹ <http://www.naic.edu/~pfreire/GCpsr.html>

Table 1. Likelihood analysis results

Models	Parameter values		
LP	α	β	E_b (GeV)
	2.051(98)	0.400(69)	1.158(45)
	2.23(12)*	0.29(09)*	1.16*
PLEC	Γ	b	E_c (GeV)
	1.544(95)	1.01(14)	3.00(33)

*4FGL-DR3 values for the LP model, while no errors (numbers in parentheses) were given for E_b .

emission, with the counterpart named J1835.3–3255 in the first *Fermi* LAT source catalog (1FGL; [Abdo et al. 2010a](#)) and latter J1835.7–3258 in the fourth catalog (4FGL; [Fermi-LAT collaboration et al. 2022](#)). Based on its γ -ray spectrum and using a source distance of 10 kpc ([Harris 1996](#)), [Wu et al. \(2022\)](#) estimated a number of 1–7 MSPs in it. Motivated by these and given the detailed ephemeris for PSR J1835–3259B provided in [Gautam et al. \(2022\)](#), we carried out timing analysis of the *Fermi*-LAT data for NGC 6652. We have been able to detect γ -ray pulsations of PSR J1835–3259B. Here we report the analysis and results.

2. ANALYSIS AND RESULTS

2.1. *Fermi*-LAT Data and source model

We selected the *Fermi*-LAT Pass 8 *Front+Back* events (evclass = 128 and evtype = 3) in the energy range of 0.1–500.0 GeV within a $20^\circ \times 20^\circ$ region of interest (RoI) centered at NGC 6652 (R. A. = $18^{\text{h}}35^{\text{m}}45^{\text{s}}.502$, decl. = $-32^\circ58'15''.621$). The time range of the data was from 2008 August 04 16:29:16.8 to 2022 June 15 22:12:11.0 (UTC). We excluded the events with zenith angles $> 90^\circ$ to avoid the contamination from the Earth’s limb and those with quality flags of ‘bad’ (by the expression DATA_QUAL >0 && LAT_CONFIG = 1), and the instrumental response function ‘P8R3 SOURCE V3’ was used. Thus high-quality data in good time intervals were selected. In the analysis, the version of Fermitools–2.0.19 packages were used.

Based on the Data Release 3 of 4FGL (4FGL-DR3; [Fermi-LAT collaboration et al. 2022](#)), which was constructed from 12-yr of LAT data, a model file was made with the script make4FGLxml.py.² The model file included the spectral parameters of the catalog sources within 25° of NGC 6652, and their spectral forms provided in 4FGL-DR3 were used. We set free the parameters of flux normalizations and spectral shapes for the

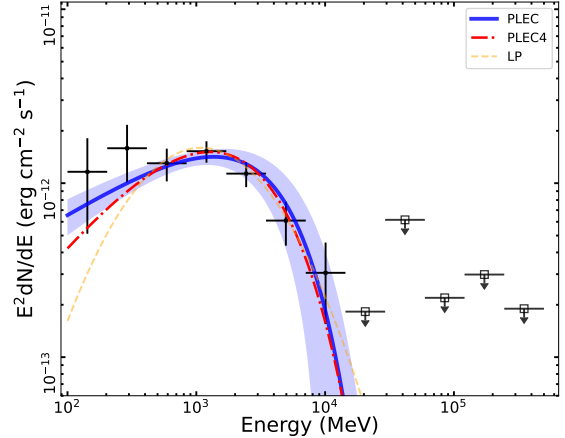


Figure 1. γ -ray spectrum in 0.1–500 GeV obtained from the data for NGC 6652. The best-fit LP and PLEC models are shown as yellow dashed and blue solid lines respectively. For the latter, its error range is also shown as the light blue region. A testing PLEC4 model is shown as the red dash-dotted line (cf., Section 2.2)

sources within 5° . Other free parameters included the normalizations of the sources within $5^\circ - 10^\circ$, those outside 10° but identified with *Variability Index* ≥ 72.44 (i.e., variable sources), and the Galactic and extragalactic diffuse emission components. All other parameters were fixed at their values provided in 4FGL-DR3.

2.2. Data analysis and spectrum extraction

A binned maximum likelihood analysis was performed to the whole LAT data, where the log-parabola (LP) model provided in 4FGL-DR3 for NGC 6652, $\frac{dN}{dE} = N_0 \left(\frac{E}{E_b}\right)^{-[\alpha + \beta \log(E/E_b)]}$, was used. The obtained best-fit parameter values are given in Table 1, which are in agreement with those given in 4FGL-DR3. The corresponding flux in 0.1–500.0 GeV was $(4.07 \pm 0.74) \times 10^{-9}$ photon $\text{cm}^{-2} \text{s}^{-1}$ and test statistic (TS) value was $\simeq 212$. Because we consider that the γ -ray emission likely arises from the MSPs, we then used the model of a power-law with an exponential cutoff (PLEC), $\frac{dN}{dE} = N_0 \left(\frac{E}{E_0}\right)^{-\Gamma} \exp[-(\frac{E}{E_c})^b]$, which is typical for describing pulsars’ γ -ray emission. Performing the likelihood analysis, the best-fit parameter values were obtained and are given in Table 1. The corresponding flux in 0.1–500 GeV was $(5.71 \pm 0.84) \times 10^{-9}$ photon $\text{cm}^{-2} \text{s}^{-1}$ and TS value was ~ 208 . As this TS value is only slightly smaller than that from the LP model, the two models (shown in Figure 1) should be considered equally good for fitting the γ -ray emission of NGC 6652. As in 4FGL-DR3, a new parameterization was developed for fitting emission of pulsars, we tested the model, PLEC4 (see

² <https://fermi.gsfc.nasa.gov/ssc/data/analysis/user/>

Fermi-LAT collaboration et al. 2022 for details), and the results were similar to that from PLEC (cf., Figure 1).

We adopted the PLEC model in the following analysis, and the obtained best-fit parameters were saved in the source model. Using the best-fit parameters of the PLEC, the integrated energy flux was calculated to be $(4.71 \pm 0.39) \times 10^{-12}$ ergs cm⁻² s⁻¹, and considering the newly reported source distance 9.46 ± 0.14 kpc for the GC (Baumgardt & Vasiliev 2021), the γ -ray luminosity (assuming isotropic emission) is $L_\gamma = (5.04 \pm 0.44) \times 10^{34}$ erg s⁻¹.

Based on the updated source model, in which the parameters of spectral shapes for all the sources were fixed at their best-fit values obtained above and the normalizations of the sources within 10° of the target and the two background components were set as free parameters, we performed spectral analysis. The 0.1–500.0 GeV energy range was divided into 12 equal logarithmically-spaced energy bins. A spectrum of the whole LAT data was extracted by performing the maximum likelihood analysis to the data in each energy bins. The obtained spectrum is shown in Figure 1, for which we kept the flux data points with TS values ≥ 4 and showed 95% flux upper limits otherwise. This spectrum is relatively well described by the PLEC model, whose Γ is within and E_c is slightly higher than the respective ranges determined from the spectra of 104 γ -ray MSPs (Wu et al. 2022).

2.3. Timing Analysis

We selected the events within an aperture radius of 6 degrees (the 68% containment angle at 0.1 GeV³) in 0.1–500 GeV band, and assigned weights to them with their probabilities of originating from the target (using the *Fermi* tool `gtsrcprob`). Pulse phases were assigned to the weighted photons based on the given ephemeris (Gautam et al. 2022) by employing Tempo2 (Hobbs et al. 2006) with *Fermi* plug-in (Ray et al. 2011). The two-dimensional phaseogram and folded pulse profile in 16 phase bins are plotted in Figure 2 (Panel B and A respectively), where the uncertainties of the counts in each bins were estimated using the method provided in Abdo et al. (2013). The pulse profile shows a peak at phase ~ 0.31 – 0.44 , as the results of the photons with large weights (high probabilities) mostly located within phase 0.3–0.5, and also a mini-peak at phase ~ 0.94 – 1.0 . A high similarity to the shape of the radio pulse profile (Panel D of Figure 2, which was approximately drawn based on that reported in Gautam et al. 2022) is thus

seen. Following Abdo et al. (2013), we estimated the background counts (diffuse emission plus contributions from the nearby sources), and the value was 89.5, equal to the lowest one (89.3 ± 2.4) of the pulse bins.

We applied the H-test statistic to the weighted photons (de Jager & Büsching 2010; Kerr 2011), and the cumulative H-test value curve over the time span of the LAT data is shown in Panel C of Figure 2. The H-test value of the whole data was $\simeq 41$, corresponding to a p -value of 7.5×10^{-8} ($\simeq 5.4\sigma$).

2.4. Phase-resolved analysis

Given the established pulse profile, we first performed the likelihood analysis to the data of the P₁ and P₂ phase ranges shown in Figure 2, for further investigation of the emissions of the pulse peaks. Using the PLEC model, the fits to the main pulse peak (P₁) and the mini-peak (P₂) were obtained. The best-fit parameters are consistent with those obtained from the whole data but with large uncertainty ranges, since the TS values were $\simeq 119$ and $\simeq 33$ respectively.

We also performed the analysis to the data of the P_{1b} and P_{off} phase ranges (Panel A of Figure 2), for checking the contributions of the major pulsed emission and the possible off-pulse emission respectively. Likelihood analysis resulted in TS values of 189 and 1 respectively. The flux upper limit (95%) for the latter was $\simeq 6.0 \times 10^{-10}$ photon cm⁻² s⁻¹ (or $\sim 5.3 \times 10^{33}$ erg s⁻¹ at the GC’s distance and assuming the PLEC parameters of the MSP).

3. DISCUSSION

By using the ephemeris given by the radio detection of PSR J1835–3259B, we have analyzed the *Fermi*-LAT data collected for NGC 6652 for approximately 14 years and detected the pulsations of this newly discovered MSP at a 5.4σ confidence level. The high similarity of the γ -ray pulse profile with the radio one also strongly supports our detection. This pulsar has a maximum spin-down rate \dot{P} of 6.65×10^{-20} (Gautam et al. 2022), which implies a spin-down luminosity of $\dot{E} \leq 4.3 \times 10^{35}$ erg s⁻¹. The γ -ray efficiency would be $\eta = L_\gamma / \dot{E} \gtrsim 0.12$ when we assign the observed L_γ to the MSP. The η value is in line with those of other MSPs (e.g., Wu et al. 2022), again supporting the detection.

Wu et al. (2022) have estimated 1–7 MSPs, with 4 MSPs as the likely case, in NGC 6652. However, the background light curve matches the pulse phase bin of the lowest counts and the results from the phase-resolved analysis indicate that the major pulsed part contributes to most of the observed γ -ray emission from the GC, strongly suggesting little contributions from

³ https://www.slac.stanford.edu/exp/glast/groups/canda/lat_Performance.html

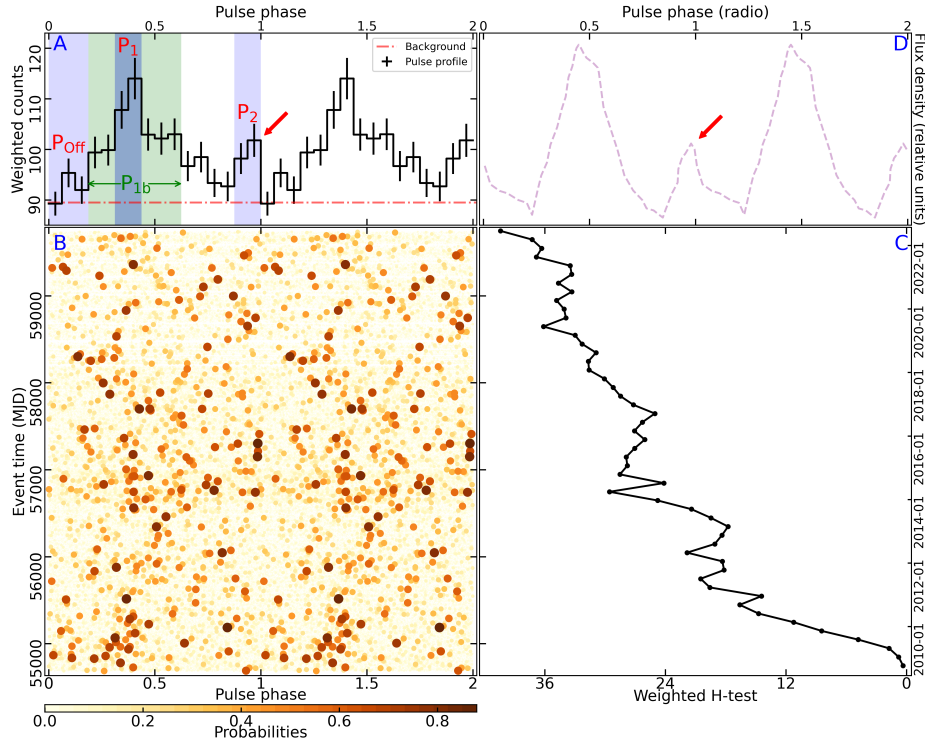


Figure 2. Timing analysis results for PSR J1835–3259B. Panel A: the integrated weighted γ -ray pulse profile (16 phase bins). Panel B: two-dimensional phaseogram (16 phase bins), where the bottom color bar indicates the weights of the photons (with the largest being 88%). Panel C: H-test values over the span of the data. Panel D: schematic radio pulse profile of PSR J1835–3259B drawn from that reported in [Gautam et al. \(2022\)](#) for comparison. Red arrows indicate the mini-peak seen in both γ -rays and radio.

other sources. We note that the first MSP J1835–3259A had no reported \dot{P} (set to zero in [DeCesar et al. 2015](#)), which thus likely contributes little to the observed γ -ray emission. [Paduano et al. \(2021\)](#) reported a candidate transitional MSP (tMSP) in the GC, which has an X-ray luminosity of $1.8 \times 10^{34} \text{ erg s}^{-1}$. If this candidate is in a sub-luminous disk state or a pulsar state, its γ -ray luminosity would be $\sim 5 \times 10^{34} \text{ erg s}^{-1}$ (i.e., $\sim L_\gamma$) or much higher respectively (based on the X-ray-to- γ -ray flux ratios summarized for tMSPs in [Miller et al. 2020](#)). The γ -ray detection of J1835–3259B actually challenges the identification of the candidate tMSP. Thus it is very likely that the γ -ray emission from the GC comes dominantly from PSR J1835–3259B.

Intriguing questions remain to be investigated such as why like NGC 6624 and NGC 6626, NGC 6652 also contains one exceptionally bright MSP. With γ -ray luminosities of $\sim 4\text{--}9 \times 10^{34} \text{ erg s}^{-1}$, the three MSPs are among the brightest ones ([Wu et al. 2022](#)). While the former two have higher spin-down luminosities of $\sim 10^{36} \text{ erg s}^{-1}$, these three all have relatively high rotational power among all MSPs. Also the former two

are isolated pulsars, but PSR J1835–3259B is in a binary likely with a Helium white dwarf companion ([Gautam et al. 2022](#)), along the evolutionary tracks for such binaries ([Tauris & Savonije 1999](#)). Further studies of pulsars in the GCs could help our understanding, by pinning down how many such bright MSPs are in the γ -ray bright GCs.

We thank anonymous referee for very helpful suggestions and W. Wu for inspiring this work and helping with the MSP property comparison. This work is supported in part by the National Key R&D Program of China under grant No. 2018YFA0404204, the National Natural Science Foundation of China No. 12163006, the Basic Research Program of Yunnan Province No. 202201AT070137, and the Foundations of Yunnan Province (202201BF070001-020). Z. W. acknowledges the support by the Original Innovation Program of the Chinese Academy of Sciences (E085021002) and the Basic Research Program of Yunnan Province No. 202201AS070005.

REFERENCES

- Abdo, A. A., Ackermann, M., Ajello, M., et al. 2009, *Science*, 325, 845
- . 2010a, *A&A*, 524, A75

- . 2010b, *ApJS*, 188, 405
- Abdo, A. A., Ajello, M., Allafort, A., et al. 2013, *ApJS*, 208, 17
- Abdollahi, S., Acero, F., Ackermann, M., et al. 2020, *ApJS*, 247, 33
- Atwood, W. B., Abdo, A. A., Ackermann, M., et al. 2009, *ApJ*, 697, 1071
- Baumgardt, H., & Vasiliev, E. 2021, *MNRAS*, 505, 5957
- Bhattacharya, D., & van den Heuvel, E. P. J. 1991, *PhR*, 203, 1
- de Jager, O. C., & Büsching, I. 2010, *A&A*, 517, L9
- de Menezes, R., Cafardo, F., & Nemmen, R. 2019a, *MNRAS*, 486, 851
- . 2019b, *MNRAS*, 486, 851
- DeCesar, M. E., Ransom, S. M., Kaplan, D. L., Ray, P. S., & Geller, A. M. 2015, *The Astrophysical Journal*, 807, L23
- Fermi-LAT collaboration, :, Abdollahi, S., et al. 2022, arXiv e-prints, arXiv:2201.11184
- Freire, P. C. C., Abdo, A. A., Ajello, M., et al. 2011, *Science*, 334, 1107
- Gautam, T., Ridolfi, A., Freire, P. C. C., et al. 2022, arXiv e-prints, arXiv:2205.15274
- Harris, W. E. 1996, *AJ*, 112, 1487
- Hobbs, G., Edwards, R., & Manchester, R. 2006, *Chinese Journal of Astronomy and Astrophysics Supplement*, 6, 189
- Hui, C. Y., Cheng, K. S., Wang, Y., et al. 2011, *ApJ*, 726, 100
- Johnson, T. J., Guillemot, L., Kerr, M., et al. 2013, *ApJ*, 778, 106
- Kerr, M. 2011, *ApJ*, 732, 38
- Kong, A. K. H., Hui, C. Y., & Cheng, K. S. 2010, *The Astrophysical Journal*, 712, L36
- Lloyd, S. J., Chadwick, P. M., & Brown, A. M. 2018a, *MNRAS*, 480, 4782
- . 2018b, *MNRAS*, 480, 4782
- Manchester, R. N., Hobbs, G. B., Teoh, A., & Hobbs, M. 2005, *AJ*, 129, 1993
- Miller, J. M., Swihart, S. J., Strader, J., et al. 2020, *ApJ*, 904, 49
- Paduano, A., Bahramian, A., Miller-Jones, J. C. A., et al. 2021, *MNRAS*, 506, 4107
- Ray, P. S., Kerr, M., Parent, D., et al. 2011, *ApJS*, 194, 17
- Song, D., Macias, O., Horiuchi, S., Crocker, R. M., & Nataf, D. M. 2021, *MNRAS*, doi:10.1093/mnras/stab2406
- Tam, P. H. T., Kong, A. K. H., Hui, C. Y., et al. 2011, *ApJ*, 729, 90
- Tauris, T. M., & Savonije, G. J. 1999, *A&A*, 350, 928
- Wu, J. H. K., Hui, C. Y., Wu, E. M. H., et al. 2013, *ApJL*, 765, L47
- Wu, W., Wang, Z., Xing, Y., & Zhang, P. 2022, *ApJ*, 927, 117
- Yuan, M., Zheng, J., Zhang, P., & Zhang, L. 2022, *Research in Astronomy and Astrophysics*, 22, 055019
- Zhang, P. F., Xin, Y. L., Fu, L., et al. 2016, *MNRAS*, 459, 99
- Zhang, P.-F., Zhou, J.-N., Yan, D.-H., et al. 2020, *ApJL*, 904, L29
- Zhou, J. N., Zhang, P. F., Huang, X. Y., et al. 2015, *MNRAS*, 448, 3215